Main Group Chemistry Hot Paper

How to cite: *Angew. Chem. Int. Ed.* **2021**, *60*, 19397–19405
International Edition: doi.org/10.1002/anie.202106980
German Edition: doi.org/10.1002/ange.202106980

A Chemiluminescent Tetraaryl Diborane(4) Tetraanion

*Hendrik Budy, Thomas Kaese, Michael Bolte, Hans-Wolfram Lerner, and Matthias Wagner**

Abstract: *Two subvalent, redox-active diborane(4) anions, [**3**]$^{4-}$ and [**3**]$^{2-}$, carrying exceptionally high negative charge densities are reported: Reduction of 9-methoxy-9-borafluorene with Li granules without stirring leads to the crystallization of the B(sp^3)–B(sp^2) diborane(5) anion salt Li[**5**]. [**5**]$^-$ contains a 2,2′-biphenyldiyl-bridged B–B core, a chelating 2,2′-biphenyldiyl moiety, and a MeO substituent. Reduction of Li[**5**] with Na metal gives the Na$^+$ salt of the tetraanion [**3**]$^{4-}$ in which two doubly reduced 9-borafluorenyl fragments are linked via a B–B single bond. Comproportionation of Li[**5**] and Na$_4$[**3**] quantitatively furnishes the diborane(4) dianion salt Na$_2$[**3**], the doubly boron-doped congener of 9,9′-bis(fluorenylidene). Under acid catalysis, Na$_2$[**3**] undergoes a formal Stone–Wales rearrangement to yield a dibenzo[g,p]chrysene derivative with B=B core. Na$_2$[**3**] shows boron-centered nucleophilicity toward n-butyl chloride. Na$_4$[**3**] produces bright blue chemiluminescence when exposed to air.*

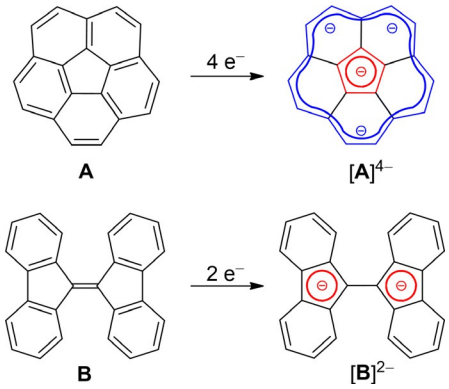

Scheme 1. Corannulene **A** and 9,9′-bis(fluorenylidene) **B** are substructures of C_{60} and are capable of reversibly accepting four and two electrons, respectively.

Introduction

Organic compounds capable of reversibly accepting multiple electrons are of fundamental interest, especially if they can be switched between antiaromatic and aromatic π-electron structures by mere electron injection. They also have a wide range of applications from redox catalysis to materials science.[1] One of the champions in the field of redox-active organics is buckminsterfullerene (C_{60}),[2–4] which can be taken from an electrically insulating neutral state through partially reduced metallic,[5] superconducting (e.g., K_3C_{60}),[6] or insulating Jahn–Teller-distorted states ($K_4[C_{60}]$)[7] to a hexaanionic form.[8,9] Some of these unique electron-accepting properties are still preserved in the fullerene fragments corannulene (**A**) and 9,9′-bis(fluorenylidene) (**B**; Scheme 1): Alkali-metal reduction leads to a tetraanion [**A**]$^{4-}$ containing two aromatic systems, one with 6 π electrons in the central C_5 ring and the other with 18 π electrons along the annulene-type C_{15} rim.[10–13] **B** readily accepts two electrons and thereby also acquires Clar's sextets[14] in its two five-membered rings.[15–21] As it turns out, the prospect of gaining aromatic character can become a strong promoter of electron uptake. A second powerful design tool is the insertion of a boron atom into the π-conjugation pathway; due to the vacant B(p_z) orbital, the result is in some ways equivalent to oxidative doping. 9-Borafluorenes combine both assets in archetypal form, since they contain a 4π-antiaromatic central borole ring that can be converted to a 6π-aromatic system by two-electron reduction.[22–24]

In the recent past, we have investigated in detail the alkali-metal reduction of the 9*H*-9-borafluorene dimer (**1**)$_2$ or of the THF adduct **1**·thf (Scheme 2).[25–34] Specifically, we found that treatment of **1**·thf with an excess of Li granules in THF leads to a product mixture from which Li$_2$[**2**], a doubly boron-doped analogue of dibenzo[*g*,*p*]chrysene (**C**), could be isolated in approximately 45% yield (Scheme 2).[35] A second major product is the borafluorene-dianion salt Li$_2$[**1**] (approx. 35%). High-yield syntheses of M$_2$[**1**] (M = Li–K) were developed in the meantime and the role of [**1**]$^{2-}$ as boron-centered nucleophile was established.[23,30–33] We have now succeeded in identifying a third reaction product, the unique tetraanion salt Li$_4$[**3**] (approx. 5%; Scheme 2). [**3**]$^{4-}$ can be regarded as composed of two dehydrogenatively coupled dianions [**1**]$^{2-}$ that communicate electronically via a direct B–B bond. Isoelectronic species that have already received considerable attention are the 9,9′-bis(fluorenylidene) dianion [**B**]$^{2-}$ (E = C),[15–21] its heavier homologues with E = Si or Ge,[21,36] and neutral 9,9′-bicarbazyl **D** (E = N; Scheme 2).[37] [**3**]$^{4-}$ accumulates a high negative charge on a relatively small molecule. Tetraanionic organoboranes are

[*] M. Sc. H. Budy, Dr. T. Kaese, Dr. M. Bolte, Dr. H.-W. Lerner, Prof. Dr. M. Wagner
Institut für Anorganische Chemie
Goethe-Universität Frankfurt
Max-von-Laue-Strasse 7, 60438 Frankfurt (Main) (Germany)
E-mail: Matthias.Wagner@chemie.uni-frankfurt.de
Supporting information and the ORCID identification number(s) for the author(s) of this article can be found under: https://doi.org/10.1002/anie.202106980.

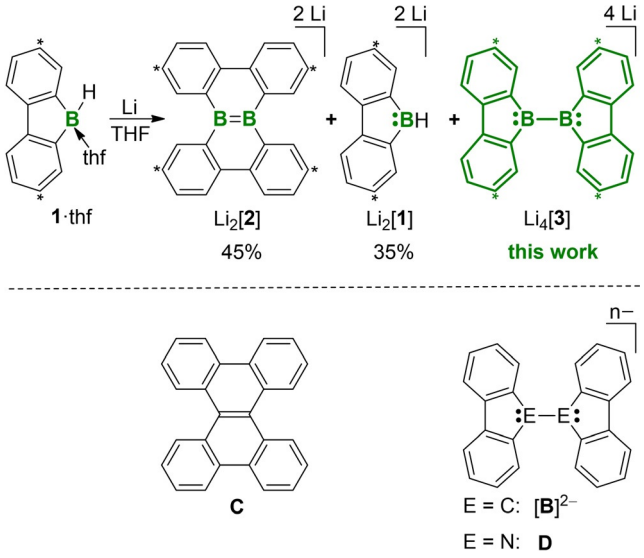

Scheme 2. Reduction of **1**·thf with an excess of elemental Li furnishes a complex mixture containing the subvalent boron species Li_2[**2**], Li_2[**1**], and Li_4[**3**] (carbon atoms marked with asterisks bear *t*Bu substituents). Isoelectronic compounds suitable for comparison are dibenzo[*g*,*p*]chrysene **C**, the 9,9′-bis(fluorenylidene) dianion $[\mathbf{B}]^{2-}$, and 9,9′-bicarbazyl **D**.

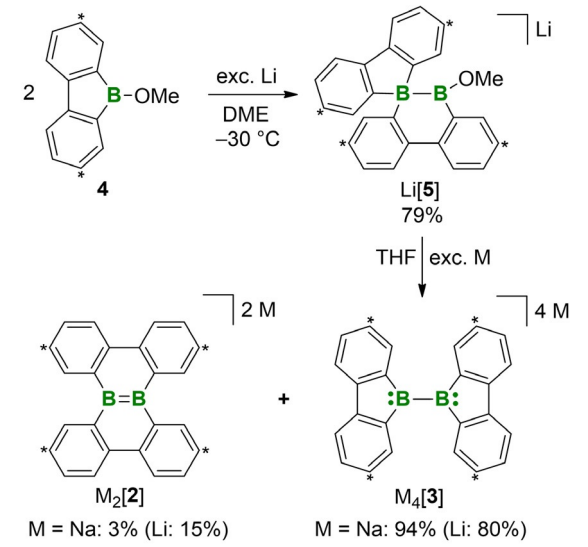

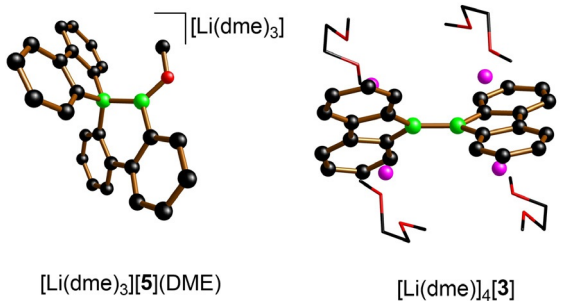

Scheme 3. Top: The B(sp^3)—B(sp^2) diborane(5) salt Li[**5**] is obtained by low-temperature lithium reduction of **4**. Further alkali-metal reduction gives a mixture of M_4[**3**] and M_2[**2**]; for M = Na, the M_2[**2**] contamination is negligible (carbon atoms marked with asterisks bear *t*Bu substituents). Bottom: Solid-state structures of [Li(dme)$_3$][**5**](DME) and [Li(dme)]$_4$[**3**] (non-coordinating DME, the *t*Bu groups, and all H atoms are omitted for clarity). Bond lengths [Å] of [Li(dme)$_3$][**5**](DME): B—B = 1.703(4), B—O = 1.374(3). Bond length [Å] and dihedral angle [°] of [Li(dme)]$_4$[**3**]: B—B = 1.705(8); $C_2B//B'C'_2$ = 47.0(3).

as yet unknown and even remotely comparable species hosting such high charge density are rare.[38]

Herein we report an optimized high-yield synthesis of the tetraanion salt Na_4[**3**] and provide a mechanistic proposal for its formation. Na_4[**3**] is unique among all other organoboron compounds in that it emits intense blue light upon contact with ambient air, thus representing an entirely new class of chemiluminescent molecules. The controlled two-electron oxidation of Na_4[**3**] gives the 9,9′-bis(borafluorenylidene) Na_2[**3**], a doubly boron-doped analogue of compound **B** and an important but previously elusive isomer of $[\mathbf{2}]^{2-}$. Factors that trigger the skeletal rearrangement of $[\mathbf{3}]^{2-}$ to $[\mathbf{2}]^{2-}$ are elucidated and juxtaposed with the conditions under which the widely investigated isomerization of the carbonaceous **B**/**C** couple occurs.

Results and Discussion

Synthesis and characterization of Na_4[3] and Na_2[3]: After screening various solvents, reaction temperatures, and boron-bonded substituents,[39] we found that stirring the 9-methoxy-9-borafluorene **4** with an excess of Li granules in 1,2-dimethoxyethane (DME) at −30 °C gave the highest ratio Li_4[**3**]:Li_2[**2**] = 1:0.3 and only small amounts of side products. However, the actual breakthrough toward selective synthesis of $[\mathbf{3}]^{4-}$ was the observation that carrying out the low-temperature reduction without stirring led to crystallization of the intermediate [Li(dme)$_3$][**5**](DME) in 79% yield (Scheme 3).[40] Subsequent room-temperature reduction of the thus purified Li[**5**] with Li or Na metal in [D_8]THF was monitored by in situ ^{1}H NMR spectroscopy.[39] Na metal proved to be the superior reducing agent, which gave the dark brown target compound Na_4[**3**] in near quantitative yield and with very low Na_2[**2**] contamination (approx. 3%; Scheme 3).[41]

The crystal lattice of [Li(dme)$_3$][**5**](DME) contains C_1-symmetric $[\mathbf{5}]^-$ anions (Scheme 3). One chelating and one bridging 2,2′-biphenyldiyl moiety create a B(sp^3)—B(sp^2) diborane(5) framework.[42,43] Single crystals of a Na_4[**3**] solvate were grown from THF, and an X-ray analysis confirmed the proposed molecular structure of the $[\mathbf{3}]^{4-}$ tetraanion.[39] However, crystals of [Li(dme)]$_4$[**3**], obtained in our above-mentioned reduction experiments on **1**·thf, possessed superior quality and were therefore chosen as the basis for discussion of structural parameters. [Li(dme)]$_4$[**3**] adopts C_2 symmetry in the solid state. All four $[Li(dme)]^+$ counter cations form contact-ion pairs with the $[\mathbf{3}]^{4-}$ unit and reside above and below the centroids of the two C_4B rings, consistent with a large accumulation of negative charge on these fragments. The tetraanion shows the structural motif of a 9,9′-bis(bora-

fluorenyl) with trigonal-planar boron centers that are connected through a direct B–B bond (Scheme 3). The respective bond length of 1.705(8) Å is remarkably similar to those in neutral tetraaryl diboranes(4).[44,45] Thus, the Coulomb repulsion of the four negative charges in $[\mathbf{3}]^{4-}$ does not appear to cause a substantial B–B-bond elongation, although the dihedral angle $C_2B//B'C'_2$ is only 47.0(3)°, similar to the case of its carbonaceous analogue $[Li(tmeda)]_2[\mathbf{B}]$ (47.8°).[16,46]

The $[\mathbf{3}]^{4-}$ scaffold exhibits pronounced bond-length alternations within its benzene rings; specifically, the peripheral rims adopt a butadiene-like character. In comparison, the three C–C bond lengths within the central C_4B ring are more equal. Taken together, these structural features indicate some aromatic delocalization of the added electrons in the five-membered rings.[47] The ^{11}B NMR spectrum ([D$_8$]THF) of $Na_4[\mathbf{3}]$ is characterized by one resonance at $\delta(^{11}B) = 14.3$ ppm, which means a downfield shift of $\Delta\delta \approx 10$ ppm compared to $Na_2[\mathbf{1}]$ ($\delta(^{11}B) = 3.9$ ppm).[31] Yet, the boron nuclei are still remarkably well shielded for tricoordinated boron centers.

With $Na_4[\mathbf{3}]$ in hand, we next targeted its two-electron oxidation to generate the dianionic diborane(4) $[\mathbf{3}]^{2-}$, a doubly boron-doped analogue of 9,9′-bis(fluorenylidene) **B** and skeletal isomer of $[\mathbf{2}]^{2-}$. Due to the extreme proneness of $Na_4[\mathbf{3}]$ to oxidation,[39] even the anionic precursor $[\mathbf{5}]^-$ is a suitable oxidizing agent: $M_2[\mathbf{3}]$ formed quantitatively in a comproportionation reaction between $Na_4[\mathbf{3}]$ and Li[**5**] (Scheme 4).[41] The product was isolated by crystallization in the form of its sodium salt $[Na(dme)_2]_2[\mathbf{3}]$, which consists of twisted $[\mathbf{3}]^{2-}$ dianions with a dihedral angle $C_2B//B'C'_2 = 25.4(2)°$ (Scheme 4).[48] The two boron atoms of $[\mathbf{3}]^{2-}$ are located at a distance of 1.637(7) Å, which is shorter by 0.068 Å than in $[\mathbf{3}]^{4-}$ and close to the corresponding values in diborane(4) dianions with firmly established B=B double bonds.[49–51] Upon going from $[\mathbf{3}]^{4-}$ to $[\mathbf{3}]^{2-}$, the B–C bonds are expanded (from av. 1.549 Å to av. 1.590 Å) and the C–C bond-length alternation within all four aryl rings is significantly diminished. The overarching picture emerging from X-ray crystallography on $[Na(dme)_2]_2[\mathbf{3}]$ is that of four aromatic Clar's sextets and a largely isolated central B=B double bond, η^2-coordinated by two complex counter cations. The general signal patterns in the ^1H and $^{13}C\{^1H\}$ NMR spectra ([D$_8$]THF) of $Na_2[\mathbf{3}]$ and $Na_2[\mathbf{2}]$ are the same, but the individual chemical shift values are distinctly different, which fits to the presence of isomeric structures that differ only in their aryl–aryl connectivities.

For the two isoelectronic pairs, boron-doped $[\mathbf{3}]^{2-}/[\mathbf{3}]^{4-}$ vs. carbonaceous $\mathbf{B}/[\mathbf{B}]^{2-}$, we next examined the differences in the distributions of the two added π electrons. $^{13}C\{^1H\}$ NMR spectroscopy was chosen as the diagnostic tool because the shielding of a specific arene carbon atom increases linearly with the π-electron density at that position and is largely unaffected by the solvent employed.[52] Figure 1 shows the differences $\Delta\delta = \delta(Na_4[\mathbf{3}]) - \delta(Na_2[\mathbf{3}])$ or $\delta(Li_2[\mathbf{B}]) - \delta(\mathbf{B})$ between the ^{13}C (red disks) or ^{11}B shift values (green disk; the areas of the disks are proportional to the corresponding Δδ values). We note the following similarities between both pairs:

(i) The two additional π charges are delocalized from the central boryl anions/carbanions into the phenylene rings. The additional shielding per phenylene ring amounts to $\Sigma(\Delta\delta) = -68.2$ ppm in $Na_4[\mathbf{3}]$ and −66.1 ppm[53,54] in $Li_2[\mathbf{B}]$.

(ii) Shielding of the two carbon atoms *ortho* to B or C-9 in $[\mathbf{3}]^{4-}$ or $[\mathbf{B}]^{2-}$, respectively, is distinctly different. This is likely due to the presence of nodal planes running close to the less shielded *ortho*-carbon atoms in the LUMOs of $[\mathbf{3}]^{2-}/\mathbf{B}$ and HOMOs of $[\mathbf{3}]^{4-}/[\mathbf{B}]^{2-}$.[16,39]

(iii) The *meta*-carbon atoms receive little additional electron density from the exocyclic π donors (note again the influence of the nodal plane).

There is also an important difference between the pairs $[\mathbf{3}]^{2-}/[\mathbf{3}]^{4-}$ and $\mathbf{B}/[\mathbf{B}]^{2-}$: A significant imbalance in the additional π electron densities on *para*-C relative to *ipso*-C of $[\mathbf{B}]^{2-}$ contrasts with a much more balanced situation in $[\mathbf{3}]^{4-}$. Plausible reasons are lower electronegativity of B vs. C and the more diffuse p_z orbital of the B(sp^2) center vs. the corresponding C(sp^2) center.

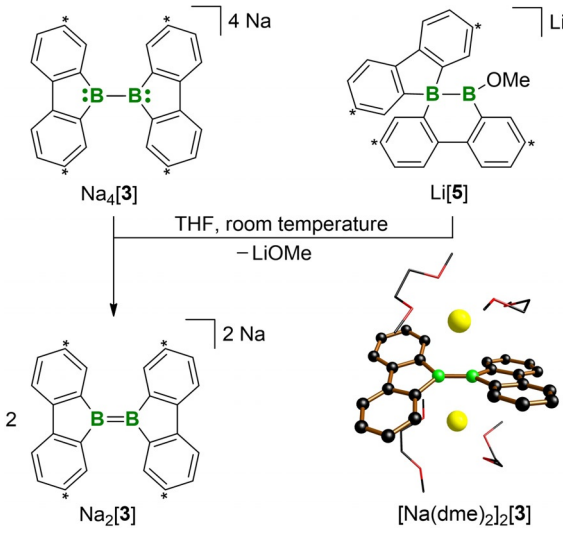

Scheme 4. Comproportionation of $Na_4[\mathbf{3}]$ with Li[**5**] yields the diborane(4)-dianion salt $Na_2[\mathbf{3}]$ (carbon atoms marked with asterisks bear *t*Bu substituents). Solid-state structure of $[Na(dme)_2]_2[\mathbf{3}]$ (the *t*Bu groups and all H atoms are omitted for clarity); bond length [Å] and dihedral angle [°]: B–B = 1.637(7); $C_2B//B'C'_2 = 25.4(2)$.

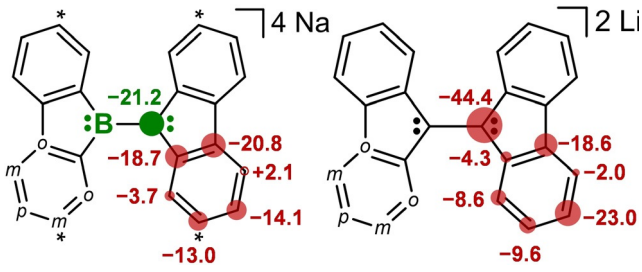

Figure 1. Chemical shift differences $\Delta\delta = \delta(Na_4[\mathbf{3}]) - \delta(Na_2[\mathbf{3}])$ (left) or $\delta(Li_2[\mathbf{B}]) - \delta(\mathbf{B})$ (right) between corresponding signals in the ^{11}B and $^{13}C\{^1H\}$ NMR spectra of the compounds. The areas of the green (^{11}B) and red (^{13}C) disks are proportional to the respective Δδ values.

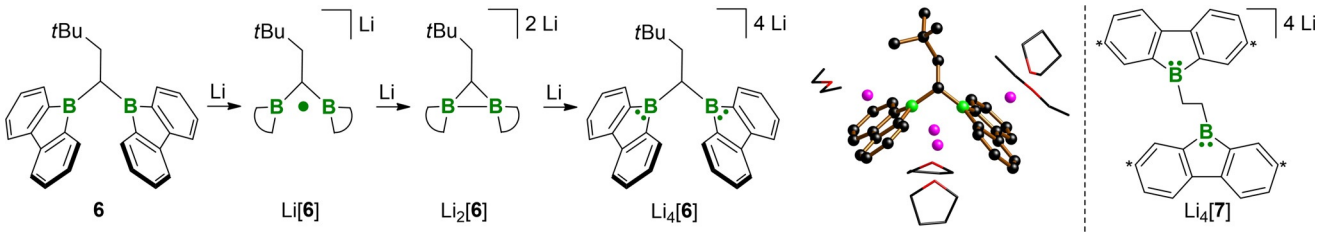

Scheme 5. Left: Stepwise reduction of **6** results in the successive build-up of one- (Li[**6**]) or two-electron bonds (Li_2[**6**]; simplified representations of the chelating 2,2′-biphenyldiyl moieties were used for Li[**6**] and Li_2[**6**]). Further injection of two electrons cleaves the B–B bond again to generate the C_1-bridged tetraanion salt Li_4[**6**]. Solid-state structure of [Li(Et_2O)][Li(thf)]$_2$[Li(thf)(Et_2O)][**6**] with all H atoms omitted for clarity. Right: The C_2-bridged tetraanion salt Li_4[**7**] (carbon atoms marked with asterisks bear *t*Bu substituents). **6**: B···B = 2.534(2) Å; Li[**6**]: B·B = 2.166(4) Å; Li_2[**6**]: B–B = 1.906(3) Å; Li_4[**6**]: B···B = 2.577(4) Å.

The high electron load of the unique tetraanion [**3**]$^{4-}$ sparked our interest in further derivatives of its kind. A promising starting material is the diborylmethane **6**[27] (Scheme 5) in which the two borafluorenyl units are no longer directly linked but separated by one C(sp^3) atom. As we had previously shown, **6** can accept one or two electrons and successively form a monoanion salt Li[**6**] with B·B one-electron two-center bond[26] and a dianion salt Li_2[**6**] with B–B two-electron two-center bond (Scheme 5).[27] In toluene, the reaction stops at this stage, even if unconsumed reducing agent is still present. However, a simple change of solvent doubles the capacity of **6** for electron uptake: Treatment of **6** or Li_2[**6**] with an excess of Li metal in THF indeed gives Li_4[**6**] in a clean reaction (Scheme 5). As a result, the B–B σ bond is reductively cleaved again. Further separation of the borafluorenyl substituents by a C_2 bridge also proved possible, yielding Li_4[**7**] (Scheme 5). The NMR and structural parameters of the borafluorenyl units in Li_4[**3**], Li_4[**6**], and Li_4[**7**] are all very similar.[39] Another lesson to be learned is that suitably preorganized bisborane platforms allow the reductive formation and subsequent reductive cleavage of B=B π bonds (cf. the [**3**]$^{2-}$/[**3**]$^{4-}$ pair) and B–B σ bonds (cf. the [**6**]$^{2-}$/[**6**]$^{4-}$ pair) and can therefore be regarded as redox switches.

*Mechanistic considerations regarding the formation of [**3**]$^{4-}$ and [**3**]$^{2-}$:* A plausible mechanistic scenario for the formation of [**3**]$^{4-}$ involves a three-step reaction sequence:

1) Formal insertion of a 9-borafluorenyl anion [**8**]$^-$ (cf. the green moieties in Scheme 6) into one B–C bond of strained **4** to give Li[**5**].[55] Similar insertions of carbenes and nitrenes, isoelectronic analogues of [**8**]$^-$, in 9-borafluorenes are well documented.[24] Transient [**8**]$^-$ could, in principle, be generated from **4** through a Li-metal reduction/LiOMe elimination sequence and could even be given some stability by DME coordination (cf. recently reported adducts of [**8**]$^-$-type species with H^- and NHC ligands).[31,47a] To test this proposal, we treated **4** with 1 equiv of Li[**2**H], which here served as a storage form of [**8**]$^-$ (Scheme 6).[23,32,33] Indeed, Li[**5**] and the byproduct **1**·thf were obtained in equimolar amounts and with perfect selectivity.[56]
2) Two-electron reduction of Li[**5**] with elimination of LiOMe to furnish [**3**]$^{2-}$ (cf. the above-mentioned comproportionation reaction Li[**5**] + Na_4[**3**]→2 M_2[**3**]; Scheme 4).

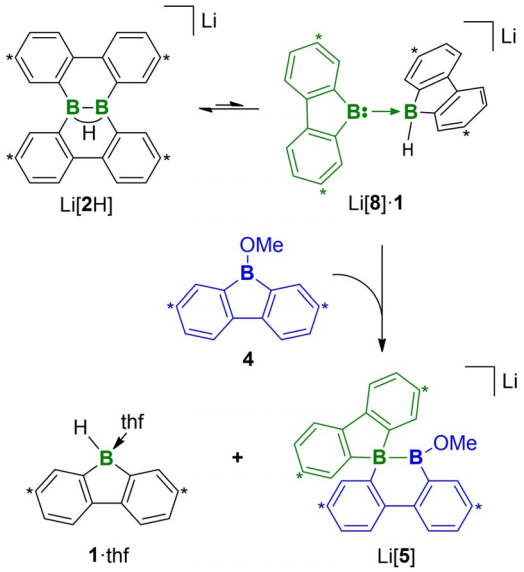

Scheme 6. Reaction of Li[**2**H] with **4** in THF gives Li[**5**] and **1**·thf, likely via the Li[**8**]·**1** adduct, which liberates a borafluorenyl anion [**8**]$^-$ (green) for insertion into one B–C bond of **4** (blue; carbon atoms marked with asterisks bear *t*Bu substituents).

3) Two-electron reduction of [**3**]$^{2-}$ to afford [**3**]$^{4-}$. In situ ^{1}H NMR monitoring of a sample containing Li[**5**] and Na metal in [D_8]THF first showed the gradual appearance of the resonances of [**3**]$^{2-}$, which then disappeared over time to give way to the signals of [**3**]$^{4-}$.[39]

The electron affinity of [**3**]$^{2-}$ distinguishes it from its isomer [**2**]$^{2-}$, which is not prone to further reduction. The differences in the redox properties are less severe between the carbonaceous analogues 9,9′-bis(fluorenylidene) (**B**) and dibenzo[*g*,*p*]chrysene (**C**): Apart from the widely documented conversion **B**→[**B**]$^{2-}$ (aromatic, stable dianion),[17,19,57–60] also the two-electron reduction of **C** to [**C**]$^{2-}$ has been described (antiaromatic, less stable dianion).[54]

A key issue is the competition between the formation of [**3**]$^{2-}$ and its isomer [**2**]$^{2-}$. On the way from [**5**]$^-$ to [**3**]$^{2-}$ the bridging 2,2′-biphenyldiyl fragment must rearrange to a chelating mode through a Wagner–Meerwein-type reaction. Alternatively, the chelating 2,2′-biphenyldiyl of [**5**]$^-$ can

undergo ring opening to become the second B···B bridging substituent in $[\mathbf{2}]^{2-}$. The outcome of the competition is influenced by the choice of alkali metal as Li yields larger amounts of $[\mathbf{2}]^{2-}$ (approx. 15%) than Na (approx. 3%). According to quantum-chemical calculations, both isomers possess comparable thermodynamic stability with $[\mathbf{3}]^{2-}$ being marginally disfavored over $[\mathbf{2}]^{2-}$ by about 2 kcal mol^{-1}.[39] However, the activation energy associated with the conversion $[\mathbf{3}]^{2-} \rightarrow [\mathbf{2}]^{2-}$ is high: Upon heating a [D$_8$]THF solution of $Na_2[\mathbf{3}]$ to 130 °C, the first clear signs of $Na_2[\mathbf{2}]$ appeared only after 1 day, and it required about 2.5 months of heating to take the reaction to completion (sealed NMR tube; ^{1}H NMR spectroscopic control). As was to be anticipated from our previous experiments, one-electron injection was also inefficient in promoting the rearrangement $[\mathbf{3}]^{2-} \rightarrow [\mathbf{2}]^{2-}$. A freshly prepared equimolar mixture of $Na_2[\mathbf{3}]$ and $Na_4[\mathbf{3}]$ gave severely broadened NMR resonances and an EPR signal (Figure S96),[39] indicating the presence of the radical intermediate $[\mathbf{3}^{\bullet}]^{3-}$. It still took about 2.5 months until only the signals of $Na_2[\mathbf{2}]$ and $Na_4[\mathbf{3}]$ remained in the spectrum (the latter compound acts as a redox catalyst and is not supposed to be consumed). In stark contrast, the $Na_2[\mathbf{3}] \rightarrow Na_2[\mathbf{2}]$ isomerization is complete within hours under acid catalysis (ethereal HCl, THF, room temperature). Concomitant ^{1}H NMR monitoring in [D$_8$]THF revealed Na[**2**H] as the primary intermediate, which is thus the actual active acid (Figure S56; cf. Scheme 7).[29,39] Since the addition of stoichiometric quantities of ethereal HCl to $[\mathbf{3}]^{2-}$ yields exclusively $[\mathbf{2}\mathrm{H}]^-$, its 9,9′-bis(borafluorenyl) isomer $[\mathbf{3}\mathrm{H}]^-$ is likely to remain elusive. Apart from NMR spectroscopy, the $Na_2[\mathbf{3}] \rightarrow Na_2[\mathbf{2}]$ conversion can be followed directly with the naked eye, as solutions of $Na_2[\mathbf{3}]$ are blue-green (λ_{onset} = 755 nm; THF) whereas those of $Na_2[\mathbf{2}]$ are red-brown (λ_{onset} = 690 nm; THF); crystals of both compounds are black with a reddish luster at the edges.[39] Electronic excitation of the carbonaceous congeners **B** (λ_{onset} = 520 nm; CH_2Cl_2)[61,62] and **C** (λ_{onset} = 396 nm; CH_2Cl_2)[63,64] requires higher energies, but the twisted fluorene isomer again shows a bathochromic shift.[65] The $[\mathbf{3}]^{2-} \rightarrow [\mathbf{2}]^{2-}$ conversion has its well-known precedence in the formal Stone–Wales rearrangement of the isoelectronic 9,9′-bis(fluorenylidene) **B** to dibenzo[*g*,*p*]chrysene **C**.[66–69] Yet, the kinetic barriers are even higher for the carbonaceous compounds.

*Chemical properties of [**3**]$^{4-}$ and [**3**]$^{2-}$. Reactivity toward HCl:* Given that protonation of $[\mathbf{3}]^{2-}$ (as well as of $[\mathbf{2}]^{2-}$) affords the familiar B–(μ-H)–B core of $[\mathbf{2}\mathrm{H}]^-$,[29] we next investigated whether the known doubly boron-doped 9,9′-bifluorenyl[28,31] $[\mathbf{3}\mathrm{H}_2]^{2-}$ can be prepared by protonation of $[\mathbf{3}]^{4-}$ (Scheme 7). Successive addition of aliquots of ethereal HCl to $Li_4[\mathbf{3}]$ in [D$_8$]THF gave no indication in the ^{1}H NMR that $Li_2[\mathbf{3}\mathrm{H}_2]$ was ever generated. Rather, we observed a redox reaction that produced $Li_2[\mathbf{3}]$, H_2,[70] and likely also $Li_3[\mathbf{3}^{\bullet}]$ (Figure S57). Note that (i) HCl titration of $Na_4[\mathbf{3}]$ was less selective and (ii) the 9,9′-bis(fluorenylidene) dianion $[\mathbf{B}]^{2-}$ and 9,9′-bifluorenyl $\mathbf{B}\mathrm{H}_2$ can cleanly be interconverted by protonation/deprotonation.[15,16,18,20]

Reactivity toward haloalkanes: Treatment of $Na_2[\mathbf{3}]$ with *n*-butyl chloride gave a quantitative conversion to the B-Cl-substitution/C–H-activation product Na[**9**] (Scheme 8). Presumably, one B atom of the B=B double bond of $Na_2[\mathbf{3}]$ is alkylated first. The resulting intermediate Na[**10**] can be regarded as adduct between a Lewis basic 9-borafluorenyl anion $[\mathbf{8}]^-$ and a Lewis acidic 9-butyl-9-borafluorene (compare the related adduct Li[**8**]·**1** in Scheme 6). In a follow-up step, $[\mathbf{8}]^-$ inserts into the C_α–H bond of the *n*-butyl chain to form Na[**9**].[30,32,33] The vigorous reactivity of $Na_2[\mathbf{3}]$ also became apparent when we tried to record cyclic voltammograms of the compound, since the initial blue-green color of the THF solution quickly faded on contact with the supporting electrolyte $[n\mathrm{Bu}_4\mathrm{N}][\mathrm{PF}_6]$. According to NMR spectroscopy, combining equimolar amounts of $Na_2[\mathbf{3}]$ and $[n\mathrm{Bu}_4\mathrm{N}][\mathrm{PF}_6]$ yields a 1:1 mixture of Na[**9**] and $n\mathrm{Bu}_3\mathrm{N}$. Apparently, the

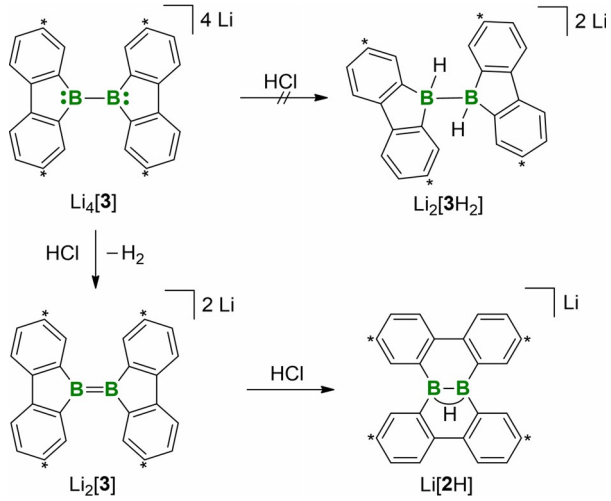

Scheme 7. Titration of $Li_4[\mathbf{3}]$ with ethereal HCl in THF does not give the diborane(6)-dianion salt $Li_2[\mathbf{3}\mathrm{H}_2]$. Rather, the diborane(4)-dianion salt $Li_2[\mathbf{3}]$ and H_2 are formed in a redox reaction. $Li_2[\mathbf{3}]$ undergoes clean protonation to Li[**2**H] (carbon atoms marked with asterisks bear *t*Bu substituents).

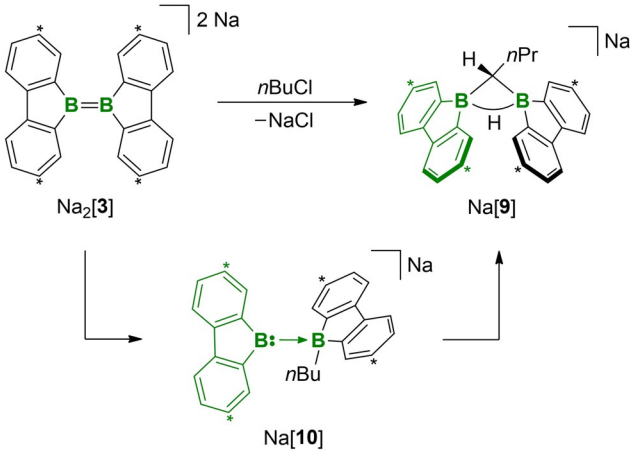

Scheme 8. The diborane(4)-dianion salt $Na_2[\mathbf{3}]$ and *n*BuCl generate Na[**9**] in a B-Cl substitution/C–H activation sequence. A borafluorenyl-anion adduct Na[**10**] is proposed as the intermediate (carbon atoms marked with asterisks bear *t*Bu substituents).

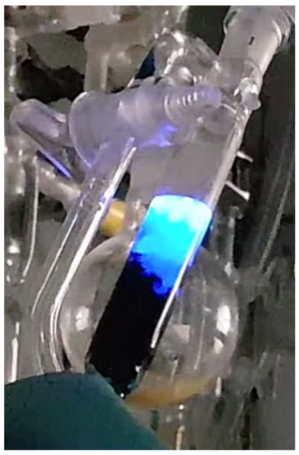

Figure 2. Intense blue chemiluminescence observed upon exposure of Li_4[**3**] to ambient air (see also the video in the Supporting Information).

$[n\mathrm{Bu_4N}]^+$ cation can take the role of the above *n*-butyl chloride, $n\mathrm{Bu_3N}$ now acting as the leaving group.[39] Treatment of Li_4[**3**] with various haloalkanes did not result in selective boron alkylation but produced complex product mixtures (K_2[**B**] and MeI furnish 9,9′-dimethyl-9,9′-bifluorenyl as the major product[21]).

Reactivity toward air: When cleaning glassware containing M_4[**3**] (M = Li, Na) with petroleum ether under ambient atmosphere, to our amazement we saw intense blue chemiluminescence (Figure 2 and the video provided in the Supporting Information). Although elucidation of the phenomenon still requires future scrutiny, the following facts can already be stated:

(i) Chemiluminescence is also observed with carefully dried air.
(ii) The addition of the peroxide $(t\mathrm{BuO})_2$ to a THF solution of M_4[**3**] under inert conditions results in non-radiative oxidation.
(iii) M_2[**1**], M_2[**2**], and M_2[**3**] are degraded by air without visible luminescence.
(iv) An ^{1}H NMR spectrum measured on a [D_8]THF solution immediately after the chemiluminescence of M_4[**3**] had faded, contained multiple overlapping signals and was therefore of limited diagnostic value (Figure S77). But after the complex mixture had been exposed to ambient atmosphere for several weeks, NMR spectroscopy revealed 4,4′-di-*tert*-butyl-1,1′-biphenyl as a major constituent (also confirmed by GC/MS).

We therefore conclude that the main origin of chemiluminescence should be reactions at the subvalent B_2 pair and/or the B–C bonds attached to it.[71] A significant fraction of these B–C bonds seems to have been retained after the end of chemiluminescence, resulting in unsymmetrically substituted 2,2′-biphenyl derivatives, which cause the observed multiple resonances. When the material is allowed to age in moist air, slow protodeborylation eventually releases the observed 4,4′-di-*tert*-butyl-1,1′-biphenyl.

The spectrum of the emitted light was measured inside the integrating sphere of a fluorescence spectrometer: We first prepared a THF solution of M_4[**3**] (M = Li, Na) inside a glovebox in a cuvette, which was then placed into the integrating sphere. By removing the lid from the cuvette, the reaction was started and after closing the integrating sphere, the spectrum was recorded with the excitation beam blocked by the shutter. Under such diffusion-controlled oxidation conditions the chemiluminescence lasts for several minutes (naked eye inspection). Three spectra were recorded in intervals of 3 min with qualitatively equal results for M = Li and Na. The spectra obtained on Na_4[**3**] were slightly better resolved and were therefore selected for description (Figures S101–S105): The first spectrum showed a broad band with a maximum at $\lambda_{max} = 425$ nm, in line with the blue color of the emission (cf. the qualitatively similar broad emission band of P_4 in the presence of air[72,73]). The hypsochromic onset at approximately 380 nm points toward an exothermicity of the underlying chemiluminescence reaction of ≥ 75 kcal mol^{-1}. The second spectrum consisted of a broad band on the hypsochromic side ($\lambda_{max} = 410$ nm) and several sharp, nearly equidistant emissions on the bathochromic side ($\lambda_{max} = 471$, 483, 495, 507 nm; $\Delta \approx 530$–480 cm^{-1}). The third spectrum exclusively showed 9 nearly equidistant, sharp bands in the region 362–483 nm, the most intense one at $\lambda_{max} = 409$ nm ($\Delta \approx 1030$–820 cm^{-1}). It therefore resembles emission spectra recorded on gas combustion systems,[74] while the general characteristics of the first spectrum are still reminiscent of the fluorescence from (boron-doped) polycyclic aromatic hydrocarbons.[22,75,76] The intensity of the emission increases over time (before it ultimately fades). This can either be an inherent property of the system or result from an increasing transmittance of the sample as the highly colored Na_4[**3**] is oxidatively degraded.

Conclusion

With the results reported here, we juxtapose the prominent series of organic compounds, 9,9′-bifluorenyl, 9,9′-bis(fluorenylidene), dibenzo[*g*,*p*]chrysene, and 9,9′-bis(fluorenylidene) dianion, with the complete set of their diborane analogues. 9,9′-Bis(fluorenylidene) is currently attracting attention as non-fullerene-type electron acceptor in organic photovoltaic cells or building block for singlet fission materials.[58–62,77–79] Also in this light, the doubly boron-doped congener $[\mathbf{3}]^{2-}$, capable of accepting two additional electrons to form the highly charged 9,9′-bis(borafluorenylidene) tetraanion $[\mathbf{3}]^{4-}$ in a reversible manner, is of fundamental interest. The dianion $[\mathbf{3}]^{2-}$ combines boron-centered nucleophilicity with the rare ability to perform subsequent C–H-activation reactions, whereas the reactivity of the tetraanion $[\mathbf{3}]^{4-}$ appears to be dominated by electron-transfer events. Remarkably, the oxidation of $[\mathbf{3}]^{4-}$ under ambient atmosphere is accompanied by a bright blue chemiluminescence, which adds a new type of system to the limited number of chemiluminescent functional groups hitherto represented mainly by activated esters and 1,2-dioxetane derivatives.[80,81]

Acknowledgements

The authors are grateful to Dr. Markus Braun for helpful discussions regarding measurement and interpretation of chemiluminescence reactions. We acknowledge Dr. Burkhard Endeward for EPR measurements. Open access funding enabled and organized by Projekt DEAL.

Conflict of Interest

The authors declare no conflict of interest.

Keywords: 9-borafluorene · boryl anions · chemiluminescence · redox chemistry · subvalent compounds

[1] *Polycyclic Arenes and Heteroarenes: Synthesis Properties, and Applications* (Ed.: Q. Miao), Wiley-VCH, Weinheim, **2015**.
[2] C. A. Reed, R. D. Bolskar, *Chem. Rev.* **2000**, *100*, 1075 – 1120.
[3] J. N. O'Shea, *Science* **2005**, *310*, 453 – 454.
[4] M. J. Rosseinsky, K. Prassides, *Nature* **2010**, *464*, 39 – 41.
[5] R. C. Haddon, A. F. Hebard, M. J. Rosseinsky, D. W. Murphy, S. J. Duclos, K. B. Lyons, B. Miller, J. M. Rosamilia, R. M. Fleming, A. R. Kortan, S. H. Glarum, A. V. Makhija, A. J. Muller, R. H. Eick, S. M. Zahurak, R. Tycko, G. Dabbagh, F. A. Thiel, *Nature* **1991**, *350*, 320 – 322.
[6] A. F. Hebard, M. J. Rosseinsky, R. C. Haddon, D. W. Murphy, S. H. Glarum, T. T. M. Palstra, A. P. Ramirez, A. R. Kortan, *Nature* **1991**, *350*, 600 – 601.
[7] A. Wachowiak, R. Yamachika, K. H. Khoo, Y. Wang, M. Grobis, D. H. Lee, S. G. Louie, M. F. Crommie, *Science* **2005**, *310*, 468 – 470.
[8] Q. Xie, E. Perez-Cordero, L. Echegoyen, *J. Am. Chem. Soc.* **1992**, *114*, 3978 – 3980.
[9] R. C. Haddon, *Pure Appl. Chem.* **1993**, *65*, 11 – 15.
[10] A. Ayalon, M. Rabinovitz, P.-C. Cheng, L. T. Scott, *Angew. Chem. Int. Ed. Engl.* **1992**, *31*, 1636 – 1637; *Angew. Chem.* **1992**, *104*, 1691 – 1692.
[11] I. Aprahamian, D. V. Preda, M. Bancu, A. P. Belanger, T. Sheradsky, L. T. Scott, M. Rabinovitz, *J. Org. Chem.* **2006**, *71*, 290 – 298.
[12] A. V. Zabula, A. S. Filatov, S. N. Spisak, A. Y. Rogachev, M. A. Petrukhina, *Science* **2011**, *333*, 1008 – 1011.
[13] A. Ayalon, A. Sygula, P. C. Cheng, M. Rabinovitz, P. W. Rabideau, L. T. Scott, *Science* **1994**, *265*, 1065 – 1067.
[14] T. Wassmann, A. P. Seitsonen, A. M. Saitta, M. Lazzeri, F. Mauri, *J. Am. Chem. Soc.* **2010**, *132*, 3440 – 3451.
[15] R. H. Cox, *J. Magn. Reson.* **1970**, *3*, 223 – 229.
[16] M. Walczak, G. D. Stucky, *J. Organomet. Chem.* **1975**, *97*, 313 – 323.
[17] Y. Cohen, J. Klein, M. Rabinovitz, *J. Chem. Soc. Chem. Commun.* **1986**, 1071 – 1073.
[18] H. P. S. Chauhan, H. Kawa, R. J. Lagow, *J. Org. Chem.* **1986**, *51*, 1632 – 1633.
[19] M. A. Fox, D. Shultz, *J. Org. Chem.* **1988**, *53*, 4386 – 4390.
[20] M. Stratakis, A. Streitwieser, *J. Org. Chem.* **1993**, *58*, 1989 – 1990.
[21] Y. Liu, D. Ballweg, T. Müller, I. A. Guzei, R. W. Clark, R. West, *J. Am. Chem. Soc.* **2002**, *124*, 12174 – 12181.
[22] L. Ji, S. Griesbeck, T. B. Marder, *Chem. Sci.* **2017**, *8*, 846 – 863.
[23] H. Budy, J. Gilmer, T. Trageser, M. Wagner, *Eur. J. Inorg. Chem.* **2020**, 4148 – 4162.
[24] X. Su, T. A. Bartholome, J. R. Tidwell, A. Pujol, S. Yruegas, J. J. Martinez, C. D. Martin, *Chem. Rev.* **2021**, *121*, 4147 – 4192.
[25] A. Hübner, M. Bolte, H.-W. Lerner, M. Wagner, *Angew. Chem. Int. Ed.* **2014**, *53*, 10408 – 10411; *Angew. Chem.* **2014**, *126*, 10576 – 10579.
[26] A. Hübner, A. M. Diehl, M. Diefenbach, B. Endeward, M. Bolte, H.-W. Lerner, M. C. Holthausen, M. Wagner, *Angew. Chem. Int. Ed.* **2014**, *53*, 4832 – 4835; *Angew. Chem.* **2014**, *126*, 4932 – 4935.
[27] A. Hübner, T. Kaese, M. Diefenbach, B. Endeward, M. Bolte, H.-W. Lerner, M. C. Holthausen, M. Wagner, *J. Am. Chem. Soc.* **2015**, *137*, 3705 – 3714.
[28] T. Kaese, A. Hübner, M. Bolte, H.-W. Lerner, M. Wagner, *J. Am. Chem. Soc.* **2016**, *138*, 6224 – 6233.
[29] T. Kaese, H. Budy, M. Bolte, H.-W. Lerner, M. Wagner, *Angew. Chem. Int. Ed.* **2017**, *56*, 7546 – 7550; *Angew. Chem.* **2017**, *129*, 7654 – 7658.
[30] T. Kaese, T. Trageser, H. Budy, M. Bolte, H.-W. Lerner, M. Wagner, *Chem. Sci.* **2018**, *9*, 3881 – 3891.
[31] J. Gilmer, H. Budy, T. Kaese, M. Bolte, H.-W. Lerner, M. Wagner, *Angew. Chem. Int. Ed.* **2020**, *59*, 5621 – 5625; *Angew. Chem.* **2020**, *132*, 5670 – 5674.
[32] T. Trageser, M. Bolte, H.-W. Lerner, M. Wagner, *Angew. Chem. Int. Ed.* **2020**, *59*, 7726 – 7731; *Angew. Chem.* **2020**, *132*, 7800 – 7805.
[33] T. Trageser, D. Bebej, M. Bolte, H.-W. Lerner, M. Wagner, *Angew. Chem. Int. Ed.* **2021**, *60*, 13500 – 13506; *Angew. Chem.* **2021**, *133*, 13612 – 13618.
[34] The parent 9*H*-9-borafluorene devoid of solubilizing and kinetically protecting *t*Bu substituents undergoes ring-opening oligomerization in non-donor solvents: a) review: A. Lorbach, A. Hübner, M. Wagner, *Dalton Trans.* **2012**, *41*, 6048 – 6063; b) A. Das, A. Hübner, M. Weber, M. Bolte, H.-W. Lerner, M. Wagner, *Chem. Commun.* **2011**, *47*, 11339 – 11341; c) A. Hübner, Z.-W. Qu, U. Englert, M. Bolte, H.-W. Lerner, M. C. Holthausen, M. Wagner, *J. Am. Chem. Soc.* **2011**, *133*, 4596 – 4609; d) A. Hübner, M. Diefenbach, M. Bolte, H.-W. Lerner, M. C. Holthausen, M. Wagner, *Angew. Chem. Int. Ed.* **2012**, *51*, 12514 – 12518; *Angew. Chem.* **2012**, *124*, 12682 – 12686; e) A. Hübner, A. M. Diehl, M. Bolte, H.-W. Lerner, M. Wagner, *Organometallics* **2013**, *32*, 6827 – 6833.
[35] T. Kaese, Ph.D. thesis, Goethe-Universität Frankfurt (Germany), **2018**.
[36] Y. Liu, T. C. Stringfellow, D. Ballweg, I. A. Guzei, R. West, *J. Am. Chem. Soc.* **2002**, *124*, 49 – 57.
[37] G. Boyer, R. M. Claramunt, J. Elguero, M. Fathalla, C. Foces-Foces, C. Jaime, A. L. Llamas-Saiz, *J. Chem. Soc. Perkin Trans. 2* **1993**, 757 – 766.
[38] Selected examples: a) V. R. Sandel, B. Belinky, T. Stefanik, D. Kreil, *J. Org. Chem.* **1975**, *40*, 2116 – 2120; b) K. Müllen, J. Oth, H.-W. Engels, E. Vogel, *Angew. Chem. Int. Ed. Engl.* **1979**, *18*, 229 – 231; *Angew. Chem.* **1979**, *91*, 251 – 253; c) B. C. Becker, W. Huber, K. Müllen, *J. Am. Chem. Soc.* **1980**, *102*, 7803 – 7805; d) D. H. O'Brien, D. L. Breeden, *J. Am. Chem. Soc.* **1981**, *103*, 3237 – 3239; e) A. Sekiguchi, T. Matsuo, R. Akaba, *Bull. Chem. Soc. Jpn.* **1998**, *71*, 41 – 47; f) T. Matsuo, H. Fure, A. Sekiguchi, *Bull. Chem. Soc. Jpn.* **2000**, *73*, 2129 – 2137; g) N. Treitel, M. Deichmann, T. Sternfeld, T. Sheradsky, R. Herges, M. Rabinovitz, *Angew. Chem. Int. Ed.* **2003**, *42*, 1172 – 1176; *Angew. Chem.* **2003**, *115*, 1204 – 1208; h) R. A. Baber, J. P. H. Charmant, A. J. R. Cook, N. E. Farthing, M. F. Haddow, N. C. Norman, A. G. Orpen, C. A. Russell, J. M. Slattery, *Dalton Trans.* **2005**, 3137 – 3139; i) M. Tresca, M. Higbee, N. S. Mills, *J. Org. Chem.* **2011**, *76*, 5539 – 5546; j) Y. Morita, T. Murata, A. Ueda, C. Yamada, Y. Kanzaki, D. Shiomi, K. Sato, T. Takui, *Bull. Chem. Soc. Jpn.* **2018**, *91*, 922 – 931; k) Z. Hana, L. Baia, S. Huo, J. Chen, X. Lu, *Main Group Met. Chem.* **2018**, *41*, 103 – 108; l) H. Ito, T. Murate, M. Fujisaki, R. Tsuji, Y. Morita, *ChemSusChem* **2021**, *14*, 1377 – 1387; m) Z. Zhou, Y. Zhu, Z. Wei, J. Bergner, C. Neiß, S. Doloczki, A. Görling, M. Kivala, M. A. Petrukhina, *Angew.*

Chem. Int. Ed. **2021**, *60*, 3510 – 3514; *Angew. Chem.* **2021**, *133*, 3552 – 3556.

[39] See the Supporting Information for more details. Deposition Numbers 2085650, 2085651, 2085652, 2085653, 2085654, 2085655, 2085656, 2085657, 2085658, 2085659, 2085660, 2085661, 2085662, and 2085663 contain the supplementary crystallographic data for this paper. These data are provided free of charge by the joint Cambridge Crystallographic Data Centre and Fachinformationszentrum Karlsruhe Access Structures service.

[40] Whenever a solvent molecule (THF, DME) serves as a ligand, its acronym is written in lower case letters (thf, dme). According to X-ray diffraction, the chemical composition of the single crystals as isolated from the reaction mixture is $[Li(dme)_3][\mathbf{5}](DME)$. Prolonged drying of the sample at room temperature under a dynamic vacuum results in the loss of 0.5 equiv of non-coordinated DME (^{1}H NMR spectroscopic control).

[41] X-ray analyses of crystals of $\{[Na(thf)(dme)_{0.5}]_2[Na(thf)]_{0.5}[Na]_{1.5}[\mathbf{3}]\}_2$, $[Na(thf)(dme)][Na(thf)_3{\cdot}thf][\mathbf{3}]$, and $[Na(dme)_2]_2[\mathbf{3}]$ gave no indication for the presence of Li^+ cations. We therefore assume pure Na^+ salts in all three cases.

[42] E. C. Neeve, S. J. Geier, I. A. I. Mkhalid, S. A. Westcott, T. B. Marder, *Chem. Rev.* **2016**, *116*, 9091 – 9161.

[43] For structurally related $B(sp^3)$–$B(sp^3)$ diborane(6) dianions featuring BH_2 or B(H)C≡C*t*Bu fragments in place of the BOMe fragment, see ref. [28,30].

[44] Mes_2B–B(Ph)Mes, B–B = 1.706(12) Å: A. Moezzi, M. M. Olmstead, R. A. Bartlett, P. P. Power, *Organometallics* **1992**, *11*, 2383 – 2388.

[45] $(o\text{Tol})_2B$–$B(o\text{Tol})_2$, B–B = 1.686(10)/1.695(9) Å (two crystallographically independent molecules in the asymmetric unit): N. Tsukahara, H. Asakawa, K.-H. Lee, Z. Lin, M. Yamashita, *J. Am. Chem. Soc.* **2017**, *139*, 2593 – 2596.

[46] We used the X-ray data published in this paper for the determination of the dihedral angle. However, our definition of this angle differs from that in the cited publication and consequently the values are not exactly the same.

[47] The solid-state structure of the monomeric dianion $[Na(thf)_3][Na(thf)][\mathbf{1}]$ is more consistent with an allylic CBC fragment in combination with a central C=C bond of enhanced double-bond character, see ref. [31]. Even though the experimentally observed bond-length alternations have been fully reproduced by quantum-chemical calculations on a model system of $[\mathbf{1}]^{2-}$ devoid of the *t*Bu groups, NICS and ACID calculations suggest a strongly delocalized central 6π-electron system. The same has been postulated for the monoanionic analogues of $[\mathbf{1}]^{2-}$, in which the B–H group is replaced by a B–NHC/cAAC fragment: a) K. Wentz, A. Molino, S. Weisflog, A. Kaur, D. Dickie, D. Wilson, R. J. Gilliard, *Angew. Chem. Int. Ed.* **2021**, *60*, 13065 – 13072; *Angew. Chem.* **2021**, *133*, 13175 – 13182.

[48] The analogous angle in 9,9′-bis(fluorenylidene) is 32.4°: J.-S. Lee, S. C. Nyburg, *Acta Crystallogr. Sect. C* **1985**, *41*, 560 – 567.

[49] $[Li(OEt_2)]_2[Mes_2B{=}B(Ph)Mes]$, B–B = 1.636(11) Å: A. Moezzi, M. M. Olmstead, P. P. Power, *J. Am. Chem. Soc.* **1992**, *114*, 2715 – 2717.

[50] $Li_2[\mathbf{2}]$, B–B = 1.608(4)–1.641(6) Å in various different solvates: see ref. [25,28] for the original data and ref. [23] for a more detailed discussion.

[51] $[Li(thf)]_2[(o\text{Tol})_2B{=}B(o\text{Tol})_2]$, B–B = 1.633(3) Å: S. Akiyama, K. Yamada, M. Yamashita, *Angew. Chem. Int. Ed.* **2019**, *58*, 11806 – 11810; *Angew. Chem.* **2019**, *131*, 11932 – 11936.

[52] For an arylborane/arylborane-dianion couple, see: a) C. Hoffend, M. Diefenbach, E. Januszewski, M. Bolte, H.-W. Lerner, M. C. Holthausen, M. Wagner, *Dalton Trans.* **2013**, *42*, 13826 – 13837; for selected examples of organic compounds, see: b) D. H. O′Brien, A. J. Hart, C. R. Russel, *J. Am. Chem. Soc.* **1975**, *97*, 4410 – 4412; c) N. S. Mills, E. E. Burns, J. Hodges, J. Gibbs, E. Esparza, J. L. Malandra, J. Koch, *J. Org. Chem.* **1998**, *63*, 3017 – 3022; d) R. Shenhar, R. Beust, R. E. Hoffman, I. Willner, H. E. Bronstein, L. T. Scott, M. Rabinovitz, *J. Org. Chem.* **2001**, *66*, 6004 – 6013; e) ref. [54].

[53] N. S. Mills, T. Malinky, J. L. Malandra, E. E. Burns, P. Crossno, *J. Org. Chem.* **1998**, *63*, 3017 – 3022.

[54] R. Shenhar, R. Beust, S. Hagen, H. E. Bronstein, I. Willner, L. T. Scott, M. Rabinovitz, *J. Chem. Soc. Perkin Trans. 2* **2002**, 449 – 454.

[55] W. J. Grigsby, P. Power, *Chem. Eur. J.* **1997**, *3*, 368 – 375.

[56] Nevertheless, an alternative scenario with initial B–B bond formation followed by Wagner–Meerwein rearrangement cannot be excluded, see ref. [28,31].

[57] M. Otero, E. Roman, E. Samuel, D. Gourier, *J. Electroanal. Chem.* **1992**, *325*, 143 – 152.

[58] F. G. Brunetti, X. Gong, M. Tong, A. J. Heeger, F. Wudl, *Angew. Chem. Int. Ed.* **2010**, *49*, 532 – 536; *Angew. Chem.* **2010**, *122*, 542 – 546.

[59] H. U. Kim, J. H. Kim, H. Suh, J. Kwak, D. Kim, A. C. Grimsdale, S. C. Yoon, D. H. Hwang, *Chem. Commun.* **2013**, *49*, 10950 – 10952.

[60] G. L. Eakins, M. W. Cooper, N. N. Gerasimchuk, T. J. Phillips, B. E. Breyfogle, C. J. Stearman, *Can. J. Chem.* **2013**, *91*, 1059 – 1071.

[61] S. Kawata, J. Furudate, T. Kimura, H. Minaki, A. Saito, H. Katagiri, Y. J. Pu, *J. Mater. Chem. C* **2017**, *5*, 4909 – 4914.

[62] J. Xu, A. Takai, A. Bannaron, T. Nakagawa, Y. Matsuo, M. Sugimoto, Y. Matsushita, M. Takeuchi, *Mater. Chem. Front.* **2018**, *2*, 780 – 784.

[63] R. Chaudhuri, M. Y. Hsu, C. W. Li, C. I. Wang, C. J. Chen, C. K. Lai, L. Y. Chen, S. H. Liu, C. C. Wu, R. S. Liu, *Org. Lett.* **2008**, *10*, 3053 – 3056.

[64] S. Hashimoto, T. Ikuta, K. Shiren, S. Nakatsuka, J. Ni, M. Nakamura, T. Hatakeyama, *Chem. Mater.* **2014**, *26*, 6265 – 6271.

[65] P. U. Biedermann, J. J. Stezowski, I. Agranat, *Eur. J. Org. Chem.* **2001**, 15 – 34.

[66] K. Suzuki, *Bull. Chem. Soc. Jpn.* **1962**, *35*, 735 – 740.

[67] R. W. Alder, G. Whittaker, *J. Chem. Soc. Perkin Trans. 2* **1975**, 712 – 713.

[68] R. W. Alder, J. N. Harvey, *J. Am. Chem. Soc.* **2004**, *126*, 2490 – 2494.

[69] E. E. Irace, E. Brayfindley, G. A. Vinnacombe, C. Castro, W. L. Karney, *J. Org. Chem.* **2015**, *80*, 11718 – 11725.

[70] The resonance of H_2 at $\delta(^1H) = 4.55$ ppm (G. R. Fulmer, A. J. M. Miller, N. H. Sherden, H. E. Gottlieb, A. Nudelman, B. M. Stoltz, J. E. Bercaw, K. I. Goldberg, *Organometallics* **2010**, *29*, 2176 – 2179) was detected in a separate experiment in which we treated a frozen solution of $Li_4[\mathbf{3}]$ in $[D_8]$THF with an excess of ethereal HCl. The sample was allowed to melt (and the reaction to occur) only after the NMR tube had been vacuum sealed.

[71] The two-electron reduction of 9,9′-bis(fluorenylidene) **B** in the presence of O_2/H_2O results in the formation of 9-fluorenone: ref. [57].

[72] R. J. Vanzee, A. U. Khan, *Chem. Phys. Lett.* **1975**, *36*, 123 – 125.

[73] R. J. Vanzee, A. U. Khan, *J. Phys. Chem.* **1976**, *80*, 2240 – 2242.

[74] T. Trindade, A. Ferreira, E. Fernandes, *Procedia Technol.* **2014**, *17*, 194 – 201.

[75] A. Escande, M. J. Ingleson, *Chem. Commun.* **2015**, *51*, 6257 – 6274.

[76] E. von Grotthuss, A. John, T. Kaese, M. Wagner, *Asian J. Org. Chem.* **2018**, *7*, 37 – 53.

[77] O. Y. Park, H. U. Kim, J. H. Kim, J. B. Park, J. Kwak, W. S. Shin, S. C. Yoon, D. H. Hwang, *Sol. Energy Mater. Sol. Cells* **2013**, *116*, 275 – 282.

[78] J. Conyard, I. A. Heisler, W. R. Browne, B. L. Feringa, S. Amirjalayer, W. J. Buma, S. Woutersen, S. R. Meech, *J. Phys. Chem. A* **2014**, *118*, 5961 – 5968.

[79] M. Y. Sui, Y. Geng, G. Y. Sun, J. P. Wang, *J. Mater. Chem. C* **2017**, *5*, 10343 – 10352.
[80] *Chemiluminescence and Bioluminescence: Past, Present and Future* (Ed.: A. Roda), RSC Publishing, Cambridge, **2011**.
[81] M. Vacher, I. F. Galván, B.-W. Ding, S. Schramm, R. Berraud-Pache, P. Naumov, N. Ferré, Y.-J. Liu, I. Navizet, D. Roca-Sanjuán, W. J. Baader, R. Lindh, *Chem. Rev.* **2018**, *118*, 6927 – 6974.

Manuscript received: May 25, 2021
Revised manuscript received: June 22, 2021
Accepted manuscript online: June 23, 2021
Version of record online: July 20, 2021

